Probing the Fast and Slow Components of Global Warming by Returning Abruptly to Pre-Industrial Forcing

Isaac M. Held * and Michael Winton

Geophysical Fluid Dynamics Laboratory/NOAA, Princeton NJ

Ken Takahashi

Instituto Geofisico del Peru, Lima, Peru

Thomas Delworth and Fanrong Zeng

Geophysical Fluid Dynamics Laboratory/NOAA, Princeton NJ

Geoffrey K. Vallis

Atmospheric and Oceanic Sciences Program, Princeton University, Princeton, NJ

* *Corresponding author address:* Isaac M. Held, Geophysical Fluid Dynamics Laboratory/NOAA, P. O. Box 308, Princeton, NJ 08542.

E-mail: isaac.held@noaa.gov

ABSTRACT

The fast and slow components of global warming in a comprehensive climate model are isolated by examining the response to an instantaneous return to pre-industrial forcing. The response is characterized by an initial fast exponential decay with an e-folding time smaller than 5 years, leaving behind a remnant that evolves more slowly. The slow component is estimated to be small at present, as measured by the global mean near-surface air temperature, and, in the model examined, grows to 0.4°C by 2100 in the A1B SRES scenario and then to 1.4°C by 2300 if one holds radiative forcing fixed after 2100. The dominance of the fast component at present is supported by examining the response to an instantaneous doubling of CO_2 and by the excellent fit to the model's ensemble mean 20th century evolution with a simple one-box model with no long times scales.

1. Introduction

It is informative to take a simulation of the future climate and, at several times along this trajectory, abruptly return to pre-industrial forcing. Matthews and Caldeira (2007) describe calculations of this type using a climate model of intermediate complexity, motivated by geoengineering proposals. Similar calculations with comprehensive climate models have the potential to increase our understanding of the variety of time scales involved in the climate response.

In this note, we describe such calculations for a particular model, the Geophysical Fluid Dynamics Laboratory's CM2.1. The qualitative behavior resulting from the return to pre-industrial radiative forcing is that of a fast cooling, with < 5 year relaxation time, leaving behind a much more slowly evolving component that we also refer to as "recalcitrant" since it is difficult to remove from the system by manipulating the radiative forcing. The magnitude of this remaining slow, or recalcitrant, component grows as one moves the time of the return to pre-industrial forcing to a later date.

The presumption here is that the climate exhibits no large hysteresis effects, allowing a relatively simple description of the time scales involved in the return to pre-industrial conditions. The model analyzed has no dynamic glaciers, nor does it have dynamic vegetation, two potential sources of hysteresis. We also do not consider the carbon cycle here, which has its own fast and slow components, but focus exclusively on the physical climate system's response to changing radiative forcing.

The fast responses we consider here have time scales of a few years. There are even faster responses on atmospheric relaxation times of a few months or less, stratospheric adjustment

to CO_2 being the classic example. One can define these ultra-fast responses as those that occur with fixed ocean temperature. Gregory and Webb (2008) have emphasized the significance of ultra-fast responses in the troposphere as well as the stratosphere. We treat all ultra-fast responses, stratospheric and tropospheric, as modifications to the radiative forcing, following Hansen et al. (2005).

After introducing an energy balance model with two time scales in Section 2 to help frame the discussion, we then turn to the coupled atmosphere-ocean GCM and first examine, in Section 3, the response to instantaneous doubling of CO_2, an experiment described, in particular, by Hasselmann et al. (1993) and Hansen et al. (2005). This computation serves to illustrate the sharpness of the separation of slow and fast time scales in the specific climate model that we analyze. Also in Section 3, we show that one can understand this model's 20th century global mean warming with considerable accuracy with no back effect of the slow component of the response onto the surface temperature, even though heat uptake by the ocean is clearly important in setting the magnitude of the warming. This picture is consistent with the discussion in a number of studies including Allen et al. (2000), Stott and Kettleborough (2002), Kettleborough et al. (2007), and Gregory and Forster (2008). The implication is that the slow component of the warming has not yet grown to an amplitude sufficient to alter global mean surface temperature significantly. In Section 4, we describe the experiments in which all forcing agents are abruptly returned to pre-industrial values. These confirm the current smallness of the slow component in this model, and illustrate how this slow component grows in time.

2. A simple model with two time scales

We consider a very simple model with fast and slow time scales to help fix ideas and terminology. For simplicity, we use a two-box model rather than the more common box-plus-diffusion model for incorporating heat exchange between shallow and deeper ocean layers:

$$c_F \frac{dT}{dt} = -\beta T - \mathcal{H} + \mathcal{F}, \tag{1}$$

$$c_D \frac{dT_D}{dt} = \mathcal{H}. \tag{2}$$

Here T as the global mean surface temperature perturbation, β the derivative of the outgoing flux to space with respect to T, while c_F is the heat capacity of the ocean layers that respond rapidly to the atmosphere, which one can think of as the waters reached by the surface mixed layer in its seasonal cycle. The heat exchange with the more slowly evolving ocean depths is denoted by $\mathcal{H}$. These deeper layers are characterized by a heat capacity $c_D >> c_F$, and a temperature T_D. The forcing is denoted by $\mathcal{F}$. We assume that the heat exchange is proportional to the difference between these two temperatures:

$$\mathcal{H} \equiv \gamma(T - T_D). \tag{3}$$

When T_D is small, this expression is consistent with Raper et al. (2002). In the unperturbed state $T = T_D = 0$; the equilibrium response is $T = T_D = \mathcal{F}/\beta$.

As long as $\mathcal{F}$ only varies on time scales longer than the fast relaxation time, $\tau_F \equiv c_F/(\beta + \gamma)$, we can ignore the term involving c_F in (1) and set

$$T \approx \frac{\mathcal{F} + \gamma T_D}{\beta + \gamma} \tag{4}$$

Substituting into the evolution equation for the slow component then gives

$$c_D \frac{dT_D}{dt} \approx -\frac{\beta\gamma}{\beta+\gamma} T_D + \frac{\gamma}{\beta+\gamma}\mathcal{F} \tag{5}$$

so that T_D relaxes to the equilibrium response $\mathcal{F}/\beta$ on the slow time scale

$$\tau_S \equiv \frac{c_D}{\beta}\frac{\beta+\gamma}{\gamma} \tag{6}$$

This time scale increases as the strength of the coupling between the fast and slow components, γ, decreases.

For early enough times that the slow component has not yet responded significantly, the climate can be thought of as responding to the instantaneous forcing, with a transient sensitivity replacing the equilibrium sensitivity:

$$T \approx T_F \equiv \frac{\mathcal{F}}{\beta+\gamma}. \tag{7}$$

where the subscript F refers both to fact that this response is fast, and that it is directly proportional to the forcing $\mathcal{F}$. The importance of this regime for our understanding of the 20th century warming has been emphasized by Gregory and Forster (2008). At times for which (7) is a good approximation, the committed warming, defined as the difference between the equilibrium response, holding $\mathcal{F}$ fixed, and the realized warming, is γ/β times the realized warming.

Referring to (1) and (3), if one returns $\mathcal{F}$ to zero rapidly, then T returns quickly to the value T_R, the recalcitrant warming, the surface manifestation of the slow warming of the ocean depths, given by

$$T_R = \frac{\gamma}{\beta+\gamma} T_D. \tag{8}$$

If the forcing is evolving slowly, (4) implies that the temperature T at any time is the sum of T_F and T_R as defined by (7) and (8). Therefore, the growth of T_R is a measure of the extent to which the warming would be underestimated by assuming self-similar evolution with a constant (transient) climate sensitivity. Once equilibrium is reached, the ratio of the recalcitrant to the fast response, T_R/T_F, is γ/β.

An important limitation of this model of the fast response is discussed by Williams et al. (2008) and Winton et al. (2010). As the climate evolves towards equilibrium, the spatial pattern of the warming evolves, so that the relationship between global mean surface temperature and outgoing flux to space changes. Because this evolving spatial pattern can be related to the oceanic heat uptake, Winton et al argue that a natural way of retaining the global mean perspective is by introducing an efficacy factor ϵ, for $\mathcal{H}$ in (1)[1] :

$$c_F \frac{dT}{dt} = -\beta T - \epsilon \mathcal{H} + \mathcal{F}, \tag{9}$$

$$c_D \frac{dT_D}{dt} = \mathcal{H}. \tag{10}$$

Winton et al find that the efficacy of the heat uptake, evaluated at the time of doubling in 1%/year CO_2 increase experiments, is greater than unity in almost all models, with median

[1]The underlying physical assumption is more apparent if one rearranges the first of these equations to read

$$c_F dT/dt = -\beta T - (\epsilon - 1)\gamma(T - T_D) - \mathcal{H} + \mathcal{F}$$

with the sum of the first two terms on the RHS now thought of as the parameterization of perturbations to the radiative flux at the top of the atmosphere. As the system approaches equilibrium, with $T \to T_D$, the sensitivity of the flux to the global mean surface temperature approaches β, but in the initial stages of the response,with $T_D \approx 0$, the different spatial structure of the response results in a larger flux response for a given change in global mean temperature, as measured by the extent to which $\epsilon > 1$.

value near 1.3 and reaching values as larger as 2. For our purposes, as long as we focus on the response for given T_D we can replace γ with $\epsilon\gamma$. In particular, the transient response for early times for which $T_D \approx 0$, becomes

$$T \approx T_F \equiv \frac{\mathcal{F}}{\beta + \epsilon\gamma}. \tag{11}$$

3. GCM response to an instantaneous increase in forcing and to 20th century forcing

We have generated four realizations of the experiment in which the CO_2 concentration in the atmosphere is doubled instantaneously, using GFDL's CM2.1 climate model (Delworth et al. 2006). Each experiment covers 100 years. The evolution of global mean surface air temperature is shown in the left panel of Fig. 1. The model warms rapidly, but then the warming plateaus until year 70, after which it recommences to grow slowly. The plateau occurs at a value of about 1.5K. This is the same value obtained in this model at the time of doubling in the standard experiment in which CO_2 is increased 1%/year (Stouffer 2006). The model's equilibrium climate sensitivity for doubling, as estimated from slab-ocean simulations, is roughly 3.4K. Consistent results for the equilibrium response are obtained by extrapolation from experiments in which a doubling or quadrupling of CO_2 is maintained for hundreds of years. So the system is clearly still far from equilibrium when it plateaus, and Fig. 1 shows only the initial steps of the transition to the equilibrium response.

The right hand panel focuses on the evolution over the first 20 years, showing the model's relaxation to a global mean response consistent with its transient climate sensitivity. Expo-

nential evolution with relaxation times of 3 and 5 years, asymptoting to the transient climate sensitivity of 1.5K, are also shown. A time scale of 4 years fits the model's relaxation reasonably well. In thinking of the smallness of this fast time constant, it is important to keep in mind both the effect of heat exchange with the deep ocean layers, which replaces $\tau_F = c_F/\beta$ with $c_F/(\beta+\gamma)$ in the simple model of Section 2, and the effects of an efficacy of heat uptake ϵ that is larger than unity, which reduces this time scale further to $c_F/(\beta + \epsilon\gamma)$. Our focus here is not on the precise value of this time constant, but rather on its clear separation from the longer time scales in the model. A similar response to the instantaneous increase in CO_2, with a very sharp distinction between fast and slow components of the response, is evident in the model of intermediate complexity described in Knutti et al. (2008).

The flatness of the plateau in this response is of interest, as it differs from the gradual emergence of the slow response expected from a two-box model, or a box-diffusion model. One tentative interpretation is suggested by a preliminary analysis indicating that a weakening of the Atlantic meridional overturning occurs during this plateau phase, restraining the warming, in particular by enhancing Northern Hemisphere sea ice cover. The model described by Hasselmann et al. (1993) has a hint of the same plateau structure, but this is less evident in Hansen et al. (2005). Further realizations are needed to determine the robustness of this feature. Indeed, inspection of the individual realizations shows that only 3 out of 4 display a clear plateau in their response. We defer further analysis of this feature and associated oceanic dynamics to future work.

We now check whether the simplest one-box model with $T_D = 0$ provides a good fit to the 20th century evolution produced by CM2.1. To determine this, we first need to estimate the forcing, $\mathcal{F}(t)$. For this purpose, following Hansen et al. (2005) we examine simulations

of the atmosphere/land component of the model over prescribed sea surface temperatures (SSTs) and sea-ice distributions, with and without the perturbations to the model that produce the radiative forcing over the past century (well-mixed greenhouse gases, ozone, solar irradiance, anthropogenic and volcanic aerosols, and land use changes). This technique allows the ultra-fast tropospheric responses discussed by Gregory and Webb (2008), along with the traditional ultra-fast stratospheric adjustment, to modify $\mathcal{F}$.

We take advantage of the existence of a 10-member ensemble of such simulations, using the time evolving prescribed boundary conditions from the 1870-2000 period, and using the identical forcing agents as in the CM2.1 simulations provided to the CMIP3 archive utilized by the 4th IPCC assessment. (A 10-member ensemble is overkill for this purpose, since ocean temperatures are prescribed, limiting the internal variability in the model.) Differencing the ensemble mean fluxes at the top of the atmosphere with and without perturbations in the forcing agents, the result for the net incoming flux is displayed in Fig. 2. In addition to the volcanic signals evident in this time series, there is a gradual increase over time that is dominated by the effects of greenhouse gases, with some compensation due to aerosol forcing. We also compute the analogous forcing due to doubling CO_2 in isolation by perturbing a fixed SST/sea ice model and obtain $F_{2X} = 3.48 W/m^2$ for the net flux at the top of the atmosphere in this model after the ultra-fast responses have taken place.

We set $\mathcal{F}(t)$ equal to the net flux, and solve

$$c_F \frac{dT}{dt} = -\tilde{\beta} T + \mathcal{F}. \tag{12}$$

with $\tilde{\beta} = F_{2X}/1.5°\text{K}$. From the perspective of the box model with the efficacy correction, we can think of $\tilde{\beta} = \beta + \epsilon\gamma$. We also set $c_F/\tilde{\beta} = 4$ years. In the left panel of Fig. 3, we compare

the resulting evolution of T with the global mean surface temperature obtained from the full GCM. For this purpose, we average over 5 realizations of the full model.[2]

It is evident that this simple box model provides an impressive fit to the global mean temperature evolution of the GCM. The right panel in Fig. 3 is identical to the left panel, except that we simply plot the instantaneous response to the annual mean forcing, $T = \mathcal{F}/\tilde{\beta}$. The agreement is maintained, except for the exaggerated responses to the volcanic forcing. The net response over the 20th century increases slightly. On annual time scales, the evolution of the warming over the 20th century is well approximated by the evolution of the forcing and an effective transient climate sensitivity, except for the volcanic responses for which one needs to include a memory of a few years to smooth the response. This picture is consistent with that advocated by Gregory and Forster (2008). The long time scales play little role because there is a gap between the fast and slow time scales of the response in this model, with the 20th century warming mostly falling within this gap, more or less as in the derivation of (4) for the simple two-box model.

To avoid misinterpretations, we emphasize the importance of using the transient rather than equilibrium sensitivity in this calculation. There is substantial heat being taken up by the oceans, but the results are consistent with the assumption that this uptake is proportional to the warming itself, resulting in a replacement of the equilibrium with the transient

[2]For consistency with our fixed-SST/sea ice forcing computation, before generating this figure we compute the difference in the global mean surface temperatures obtained from the prescribed SST simulations with and without changes in the radiative forcing agents, and subtract this small change from the coupled model's response. These fixed SST global mean responses, resulting from the ultra-fast land warming that manages to occur despite the fixed SSTs and sea ice, amount to less than 0.1°K in CM2.1, so the basic result in the figure is not affected by this detail, but the agreement is improved marginally.

sensitivity. In addition, despite the resulting warming of the deeper oceanic layers (and the associated sea level rise due to thermal expansion in the GCM) the global mean surface temperatures are substantially unaffected by this warming.

We prefer the concept "transient climate sensitivity", or TCS, to the more commonly used "transient climate response" or TCR, the response at the time of doubling in the standarad 1%/yr increase in CO_2. The two expressions are simply related by the radiative forcing due to CO_2 doubling: $TCS = TCR/F_{2X}$, but the key point is that TCS is also relevant for many other forcings as long as the focus is on time scales residing in the gap between the fast and slow responses. In particular, these intermediate time scales are evidently directly relevant for nearly all of the 20th century response to anthropogenic forcing.

We do not argue that there is no effect at all of the deep ocean warming on surface temperatures on these time scales. For example, a closer examination of the spatial pattern of the response to the instantaneous doubling of CO_2 uncovers changes over the 100 year time frame in Fig. 1, especially in the tropics. But these variations in spatial structure do not have a substantial effect on the global mean temperature.

It may be that the separation in time scales is less clear in other comprehensive models, necessitating consideration of a more complex frequency-dependent response to explain the models' behavior over the 20th century. It is also likely that models with more substantial aerosol forcing would at least require consideration of the efficacy of the aerosol forcing in order to obtain a fit of this quality to the global mean evolution.

4. The recalcitrant component

We now describe the response of the CM2.1 model to the instantaneous return to pre-industrial forcing. We first construct a simulation of the period 1860-2300 by appending a simulation of the A1B SRES scenario for the 21st century to one of the simulations of the 1860-2000 period with estimated historical forcings. In this scenario, CO_2 increases to 720 ppm by 2100. We extend this integration to 2300, holding all forcing agents fixed from 2100 to 2300. We then perform 4 additional 100 year experiments, initialized from this 1860-2300 simulation, in which the forcing agents are instantaneously returned to their 1860 values in the years 2000, 2100, 2200, and 2300. The result is shown in Fig. 4.

As a rough estimate of the magnitude of the slow, or recalcitrant, warming, we average temperatures over the years 10-30 following the switch off of the forcing. The thin black line in Fig. 4 connects these points. These estimates confirm that the recalcitrant component is still small at present, roughly 0.1K according to this GCM. In 2100 it is roughly 0.4K, and grows to 1.4K by 2300. At equilibrium, the total response is expected to be a combination of fast and recalcitrant components, with the ratio $T_R/T_F = \gamma/\beta$ in the simple model of Section 2, where γ would be replaced by $\epsilon\gamma$ in a model taking into account the efficacy of heat uptake. We estimate this ratio to be roughly unity in CM2.1 but somewhat smaller than unity in most models, based on comparisons of transient and equilibrium warmings.

The evolution after the instantaneous return to pre-industrial forcing in years 2000 and 2100 suggests the possibility of some modest overshooting and non-monotonic behavior, perhaps indicating that the slow warming has some momentum, which would require at least two effective degrees of freedom within the slow component. (We have removed an estimate

of a small drift in the control simulation from these global mean temperatures, but this behavior does not appear to be sensitive to the method used to remove this drift.) Additional realizations would be required to make a case for a more complex time-dependence. There is also a suggestion that the interannual variability of global mean temperature, dominated by ENSO, increases once the fast response is peeled away and the recalcitrant component is made visible. The evolution of ENSO in these return-to-preindustrial simulations may repay a closer examination, which we do not attempt here.

In Fig. 5, we plot the evolution over the first 20 years of the three switch-off experiments starting in 2100, 2200, and 2300. We subtract from each time series the global mean recalcitrant warming as estimated in Fig. 4. The responses are all of the same magnitude, as expected for the fast response (7), since the forcing is held fixed from 2100 to 2300. The implication is that the growth of the total response during this period is due to the growth of the recalcitrant component. The reduction in forcing that leads to this fast response is the sum of the pre-industrial-to-2000 forcing, roughly $2W/m^2$ from Fig. 2, and the 2000-2100 forcing in the A1B scenario, estimated to be $4.5W/m^2$ for this model (Table 1 in Levy et al. (2008)), for a total of about $6.5W/m^2$. Using the same value of effective sensitivity, $1.5K/(3.5W/m^2)$, used to generate the fit in Fig. 3, we expect a fast cooling of 2.8K, roughly consistent with the 2.6-2.7K range seen in these three cases.

The results are compared once again to exponential decays with time scales of 3 and 5 years in Fig. 5. In this case, the fit suggests a relaxation time closer to 3 years, somewhat shorter than that seen in the instantaneous doubling experiment. The fast early exponential relaxation helps justify the use of the 10-30 year average as the definition of the slow component.

It has been understood since the first GCM comparisons of transient and equilibrium climate change (Manabe et al. 1991) that the spatial pattern of the surface warming in transient simulations differs from the equilibrium pattern. In the initial stages of transient simulations, there is relatively more tropical warming and less polar amplification, and especially smaller warming in the Southern oceans. We expect to see this difference enhanced if we compare the pattern of the slow component with that of the fast component, since the transient warming is dominated by the fast component while the equilibrium warming is a combination of fast and slow components.

We compute the patterns of the fast and slow components around the years 2100, 2200, and 2300. The slow component is once again computed by averaging over years 10-30 after the switch off in each case, while the fast component is computed as the difference between the full A1B response, averaging over the 20 years centered on the date of the switch off, and the slow component. The zonal means of these patterns are shown in Fig. 6, normalized by the global mean in each case. We only show the fast component for the 2100, 2200, and 2300 cases, and the slow component for 2200 and 2300. The patterns are less robust for earlier times, especially for the slow component, because the forced responses are small enough that internal variability is significant. Multiple realizations would be needed to study the detailed evolution of these spatial patterns. For the cases shown, the latitudinal structure of the fast and slow responses are roughly conserved in time. As expected, the more pronounced differences between the patterns characterizing the fast and slow components are in high Southern latitudes, where the slow component is dominant in these normalized patterns, and in subtropical and middle latitudes in the Northern Hemisphere, where the normalized fast component is larger. At least at the level of detail evident in these zonal

means, there seems to be value in thinking of the response as a sum of two patterns with structures that are conserved in time.

The latitude-longitude structure of the normalized responses are shown for these same cases in Fig. 7. The cooling in the sub-polar North Atlantic is only apparent in the slow component, but weakens as time progresses (with or without normalization) despite the increase in the amplitude of the slow component. Comparison with the trend shown in Winton et al. (2010) for the forcing-stabilized section of the same integration indicates a similar pattern to that of the slow component in Fig. 7, but with no cooling in the sub-polar North Atlantic. Thus, the assumption that the response is the sum of only two distinct patterns may be a useful idealization on the level of zonal means, but of limited validity on closer inspection of the spatial structure. We suspect that an additional degree of freedom measuring the strength of the Atlantic meridional overturning circulation is needed to fit the evolution of these spatial structures.

In the tropical Pacific, the fast pattern is La-Nina-like, with maximum warming in the west, but this maximum moves to the East Pacific, becoming more El Nino-like, in the slow pattern (cf Cai and Whetton (2001)). This evolution is consistent with the mechanism described by Clement et al. (1996) as being active on fast time scales, with the eastern tropical Pacific temperatures held back by the continued upwelling of cold waters that have not yet felt the effects of warming. The normalized response in this region grows on longer time scales as the upwelling waters warm. Further inspection reveals that there is significant evolution towards the El Nino-like tropical warming pattern in the instantanenous doubling experiment of Fig. 1 over the years 20-70 during which the global mean response is temporarily equilibrated, suggesting that this pattern emerges more quickly than does the

global mean amplitude of the slow response, indicative of another limitation to a two-mode decomposition.

Amplification of the response over land is evident in the fast response, but much less so in the slow component. Lambert and Chiang (2007) describe how the ratio of warming over land and ocean is roughly constant in time in GCM simulations of the 20th century and in future projections. Our results suggest some reduction in this ratio is to be expected as the recalcitrant component of the warming becomes significant. More generally, the accuracy of the pattern scaling approximation, in which the geographical and seasonal pattern of change is held fixed and only its amplitude varies in time, is limited by the differences between these two patterns. However, the slow growth of the recalcitrant component in these simulations suggests that this limitation may be of little practical relevance for regional climate change studies confined to the next 100 years.

5. Conclusions

By analyzing a particular coupled atmosphere-ocean GCM, we conclude that it is useful to think of its global mean response to changes in radiative forcing as consisting of two components, as discussed, for example, by Hasselmann et al. (1993). One component responds very quickly to changes in forcing, with a characteristic time scale of less than 5 years, so its amplitude at any time can be thought of as determined by the values of the forcing over a few years prior to the time in question. The experiment of instantaneously returning to pre-industrial forcing, and waiting for 20 or so years for the fast component to decay, provides an operational definition of this decomposition. In the context of these return-to-pre-industrial

experiments, it is descriptive to refer to the slow component as "recalcitrant" because it responds very sluggishly to reduction of the radiative forcing.

In the GFDL/CM2.1 model analyzed here, the global mean recalcitrant component is still small (about 0.1K) at the start of the 21st century, and grows very slowly (to roughly 0.4K in 2100 in the A1B scenario). The dominance of the fast response at the end of the 20th century is confirmed, in this model simulation, by the ability to quantitatively fit the simulations up to the year 2000 with a simple model of the fast response only. The growth of the recalcitrant component is responsible for acceleration of the warming beyond what would be estimated based on the assumption that the response is proportional to the forcing. During a period of stabilized forcing, we expect the growth of the full response to be roughly equal to the growth of the recalcitrant component.

This decomposition works well for this GCM because it exhibits a very clear separation of time scales, at least from a global mean perspective, as shown by examining the response to an instantaneous doubling of CO_2. If other GCMs do not show such a well defined gap, more complex idealized frameworks will be needed to fit their behavior.

Assuming that this gap is robust, it is also relevant to other sources of forcing. For example, the response to volcanic forcing in surface temperature is considered to last for only a few years, but there is also a large response in ocean heat storage, and sea level, that persists much longer (e.g., Stenchikov et al. (2009)). This deep ocean thermal response must also eventually equilibrate, on time scales of centuries or longer, accompanied by a small but persistent surface cooling signature. As is easily illustrated by the response of the two-component model of Section 2 to impulsive cooling, the temperature signal, integrated over time scales longer than the fast response but shorter than the slow response, will

be determined by the transient climate sensitivity. Integrated over the time scale of the restoration of the deep ocean storage and sea level, the temperature signal will be determined by the equilibrium climate sensitivity. For CM2.1, one expects the latter to be roughly twice as large as the former, to the extent that differences in efficacy between volcanic and greenhouse forcings can be ignored.

The decomposition between fast and recalcitrant components of global warming is relevant for geo-engineering in a hypothetical future in which massive amounts of CO_2 can be extracted from the atmosphere. The fast component of the warming can be readily manipulated by manipulating the CO_2. One could compensate for the presence of the recalcitrant component by reducing CO_2 sufficiently so as to return to the pre-industrial global mean temperature, but because it has a different spatial structure than the fast component, one cannot return fully to the pre-industrial climate by manipulating the CO_2 except by waiting for the recalcitrant component to decay. The slow growth of the recalcitrant component, still less than 0.5°C in the global mean in the year 2100 for the A1B scenario, is, therefore, of some interest; the opportunity of returning to a close facsimile of the pre-industrial climate by developing technology to remove CO_2 from the atmosphere is lost gradually. Of course, the assumption here is that there is no loss of reversibility from such sources as glacial or vegetation dynamics. It is also worth keeping in mind that most of the sea level response due to thermal expansion will reside in the recalcitrant component.

The experiment described here, in which radiative forcing is returned abruptly to pre-industrial conditions, must be clearly distinguished from the experiment in which emissions are abruptly set to zero, as described, for example, by Solomon et al. (2009). The time scales of the physical climate, which we hope these experiments help elucidate, must be convolved

with the time scales of the carbon cycle in order to understand the response to different emissions trajectories.

Acknowledgments.

We thank Ronald Stouffer and Robert Hallberg for helpful reviews of an earlier draft. KH was supported by the NOAA Climate and Global Change Postdoctoral Fellowship Program, administered by the University Corporation for Atmospheric Reserarch (award NA06OAR4310199 from NOAA Climate Programs Office). IMH would like to acknowledge a conversation with Adam Scaife in 2008 on the time scale of the response to the instantaneous return to pre-industrial radiative forcing that helped motivate this study.

REFERENCES

Allen, M. R., P. A. Stott, J. F. M. Mitchell, P. Schnur, and T. Delworth, 2000: Quantifying the uncertainty in forecasts of anthropogenic climate change. *Nature*, **407**, 617–620.

Cai, W. and P. H. Whetton, 2001: A time-varying greenhouse warming pattern and the tropical-extratropical circulation linkage in the Pacific Ocean. *J. Climate*, **14**, 3337–3355.

Clement, A. C., R. Seager, M. A. Cane, and S. E. Zebiak, 1996: An ocean dynamical thermostat. *J. Climate*, **9**, 2190–2196.

Delworth, T., et al., 2006: GFDL's CM2 global coupled climate models. Part I: Formulation and simulation characteristics. *J. Climate*, **19**, doi:10.1175/JCLI3629.1.

Gregory, J. M. and P. M. Forster, 2008: Transient climate response estimated from radiative forcing and observed temperature change. *J. Geophys. Res.*, **113**, doi:10.1029/2008JD010405.

Gregory, J. M. and M. J. Webb, 2008: Tropospheric adjustment induces a cloud component in CO_2 forcing. *J. Climate*, **21**, 58–71.

Hansen, J. E., et al., 2005: Efficacy of climate forcings. *J. Geophys. Res.*, **110**, doi:10.1029/2005JD005776.

Hasselmann, K., R. Sausen, E. Maier-Reimer, and R. Voss, 1993: On the cold start problem in transient simulations with coupled atmosphere-ocean models. *Clim. Dyn.*, **9**, 53–61.

Kettleborough, J. A., B. B. B. Booth, P. A. Stott, and M. R. Allen, 2007: Estimates of uncertainty in predictions of global mean surface temperature. *J. Climate*, **20**, 843–855.

Knutti, R., S. Krahenmann, D. J. Frame, and M. R. Allen, 2008: Comment on "heat capacity, time constant, and sensitivity of earth's climate system. *J. Geophys. Res.*, **113**, doi:10.1029/2007JD009473.

Lambert, F. H. and C. H. Chiang, 2007: Control of land-ocean temperature contrast by ocean heat uptake. *Geophys. Res. Lett.*, **34**, doi:10.1029/2007GL029755.

Levy, H., M. D. Schwarzkopf, L. Horowitz, V. Ramaswamy, and K. L. Findell, 2008: Strong sensitivity of late 21st century climate to projected changes in short-lived air pollutants. *J. Geophys. Res.*, **113**, doi:10.1029/2007JD09176.

Manabe, S., R. J. Stouffer, M. J. Spelman, and K. Bryan, 1991: Transient response of a coupled atmosphere-ocean model to gradual changes of atmospheric CO_2. Part I: Annual mean response. *J. Climate*, **4**, 785–818.

Matthews, H. D. and K. Caldeira, 2007: Transient climate-carbon simulations of planetary engineering. *Proc. Nat. Sci. U.S.A.*, **104**, 9949–9954.

Raper, S. C. B., J. M. Grefory, and R. J. Stouffer, 2002: The role of climate sensitivity and ocean heat uptake on AOGCM transient temperature response. *J. Climate*, **15**, 124–130.

Solomon, S., G.-K. Plattner, R. Knutti, and P. Freidlingstein, 2009: Irreversible climate change due to carbon dioxide emissions. *Proc. Nat. Sci. U.S.A.*, **106**, 1704–1709.

Stenchikov, G., T. L. Delworth, V. Ramaswamy, R. J. Stouffer, A. Wittenberg, and F. Zeng, 2009: Volcanic signals in oceans. *J. Geophys. Res.*, **114**, doi:10.1029/2008JD011673.

Stott, P. A. and J. A. Kettleborough, 2002: Origins and estimates of uncertainty in predictions of twenty-first century temperature rise. *Nature*, **416**, 723–726.

Stouffer, R. J., 2006: GFDL's CM2 global coupled climate models. Part IV: Idealized climate response. *J. Climate*, **19**, doi:10.1175/JCLI3632.1.

Williams, K. D., W. J. Ingram, and J. M. Gregory, 2008: Time variation of effective climate sensitivity in GCMs. *J. Climate*, **21**, 5076–5090, doi:10.1175/2008JCLI2371.1.

Winton, M., K. Takahashi, and I. M. Held, 2010: Importance of ocean heat uptake efficacy to transient climate change - to appear. *J.Climate*.

List of Figures

5 The initial cooling after instantaneous return of all radiative forcing agents to their values in 1860, with the magnitude of the recalcitrant response subtracted. The three case, switched off in years 2100, 2200 and 2300, are nearly indistinguishable in amplitude as well as temporal evolution. Also shown for reference are exponential relaxation curves with times scales of 3 and 5 years. 29

6 Structure of the zonal mean response of surface air temperature in the recalcitrant and fast components, normalized so that the global mean of each is unity. Two computations are shown for the recalcitrant component (2200 and 2300) and three for the fast component (2100, 2200, and 2300), as simulated by CM2.1. 30

7 The spatial pattern of the surface air temperature in the recalcitrant and the fast responses, normalized to unity over the sphere, for the same cases as shown in Fig. 6. The thick contour corresponds to a warming of 1°C, separating those regions with responses larger and smaller than the global mean. 31

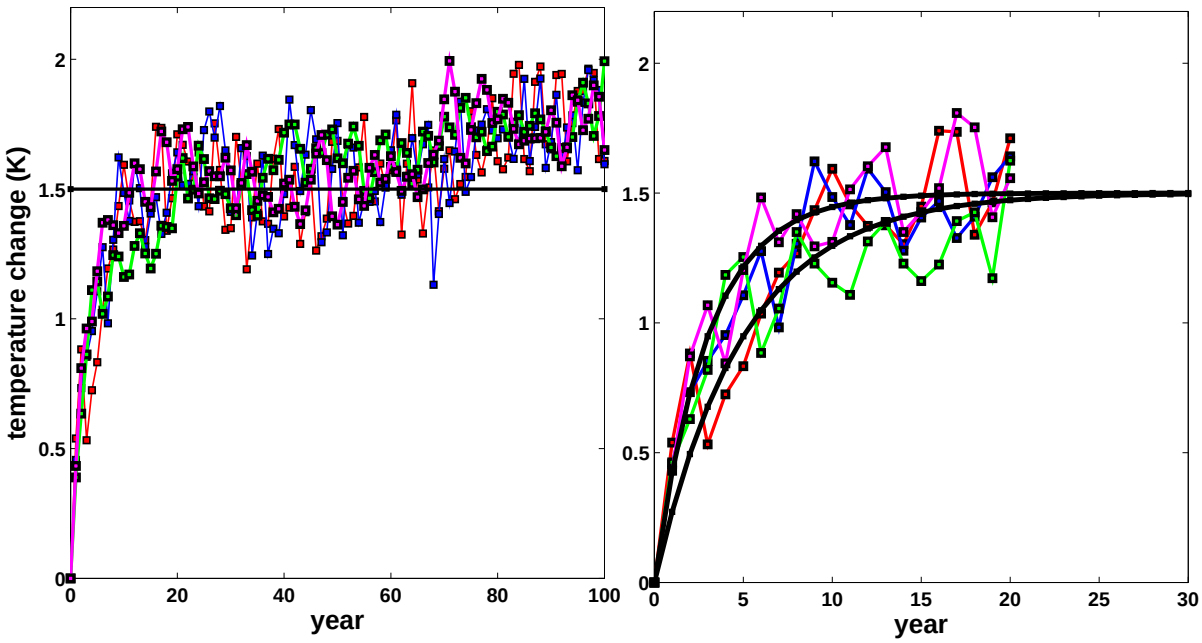

FIG. 1. Left: Four realizations of global mean near-surface air temperature in 100 year simulations of CM2.1 in response to instantaneous doubling of CO_2; Right: The first 20 years of the response, compared to exponential relaxation to the value of 1.5K with time scales of 3 years and 5 years.

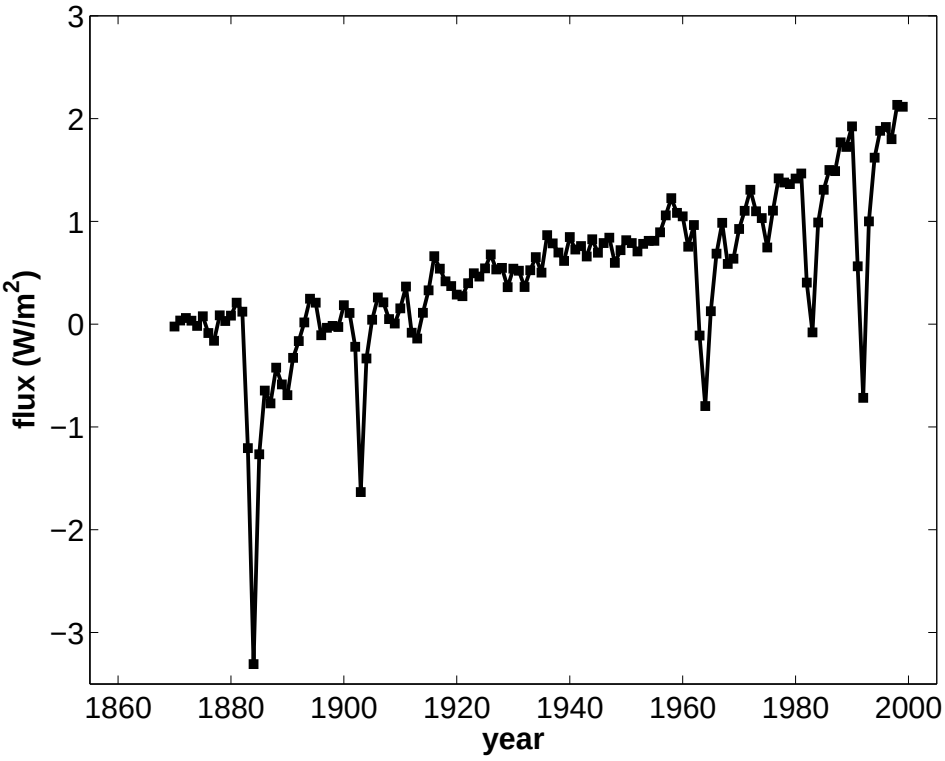

FIG. 2. The net forcing at the top of the atmosphere due to all forcing agents in CM2.1, computed as described in the text. The annual mean forcing is shown for each year.

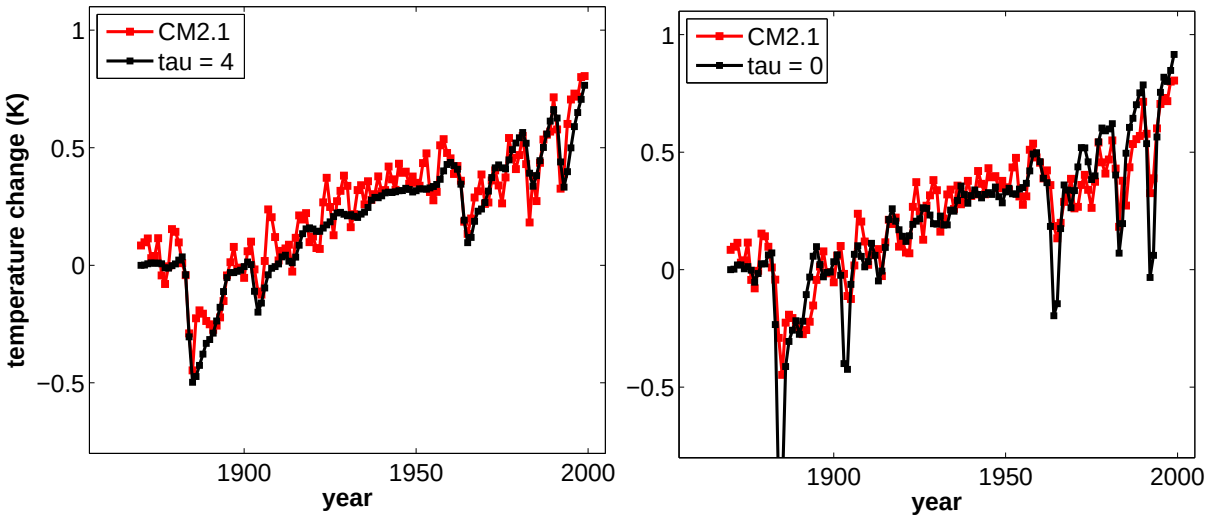

FIG. 3. Left: Fit to global mean warming of surface air temperature in CM2.1 over the 1870-2000 time period using a one-box model with an effective transient climate sensitivity and a relaxation time scale of 4 years. The GCM result is an average over a 5-member ensemble; Right: The analogous fit assuming instead an instantaneous response to the annual mean forcing, obtained by dividing the forcing by the transient climate sensitivity.

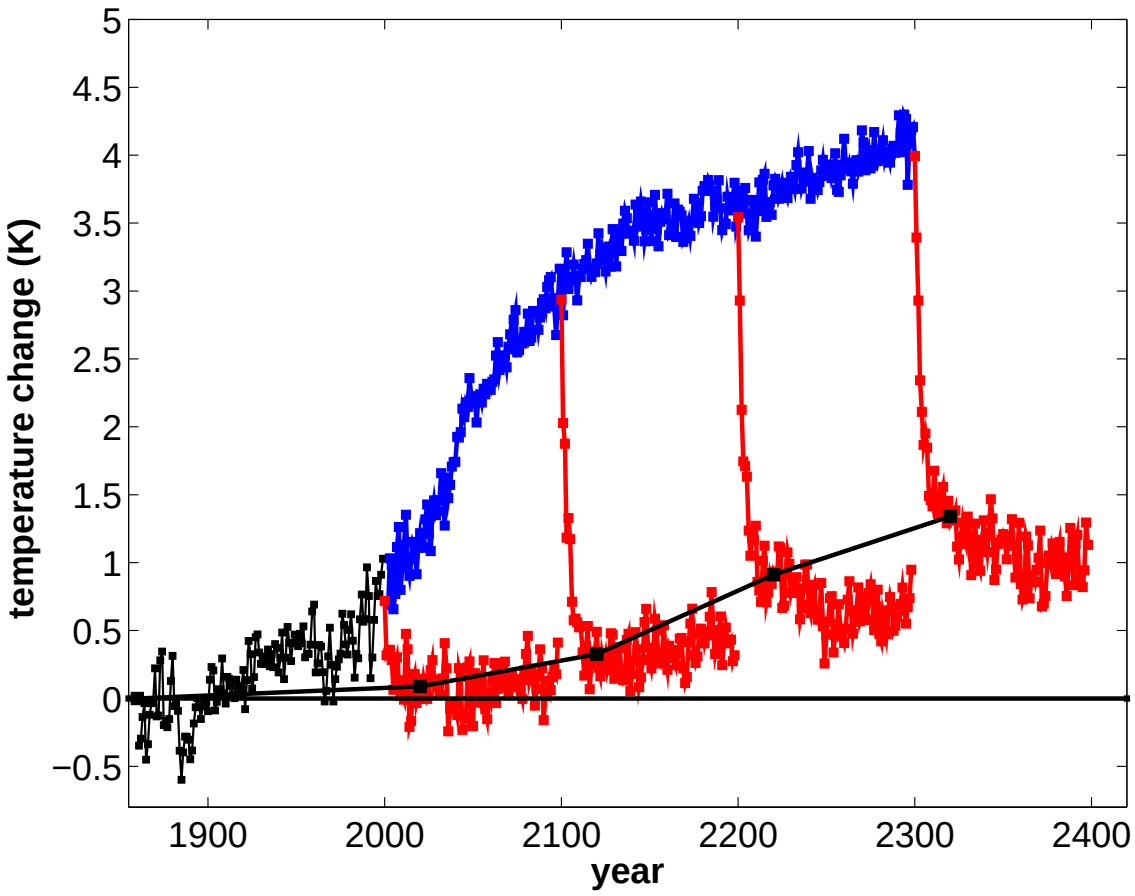

FIG. 4. The global mean surface air temperature in CM2.1 simulations with historical forcing (black), with A1B forcing, stabilized in 2100 and extended for 200 additional years with fixed forcing agents (blue), and 4 experiments in which the forcing agents are returned to their 1860 values instantaneously, in years 2000, 2100, 2200, and 2300 (red). The thin black line is an estimate of the recalcitrant component of the response, obtained by averaging over years 10-30 after the switch off.

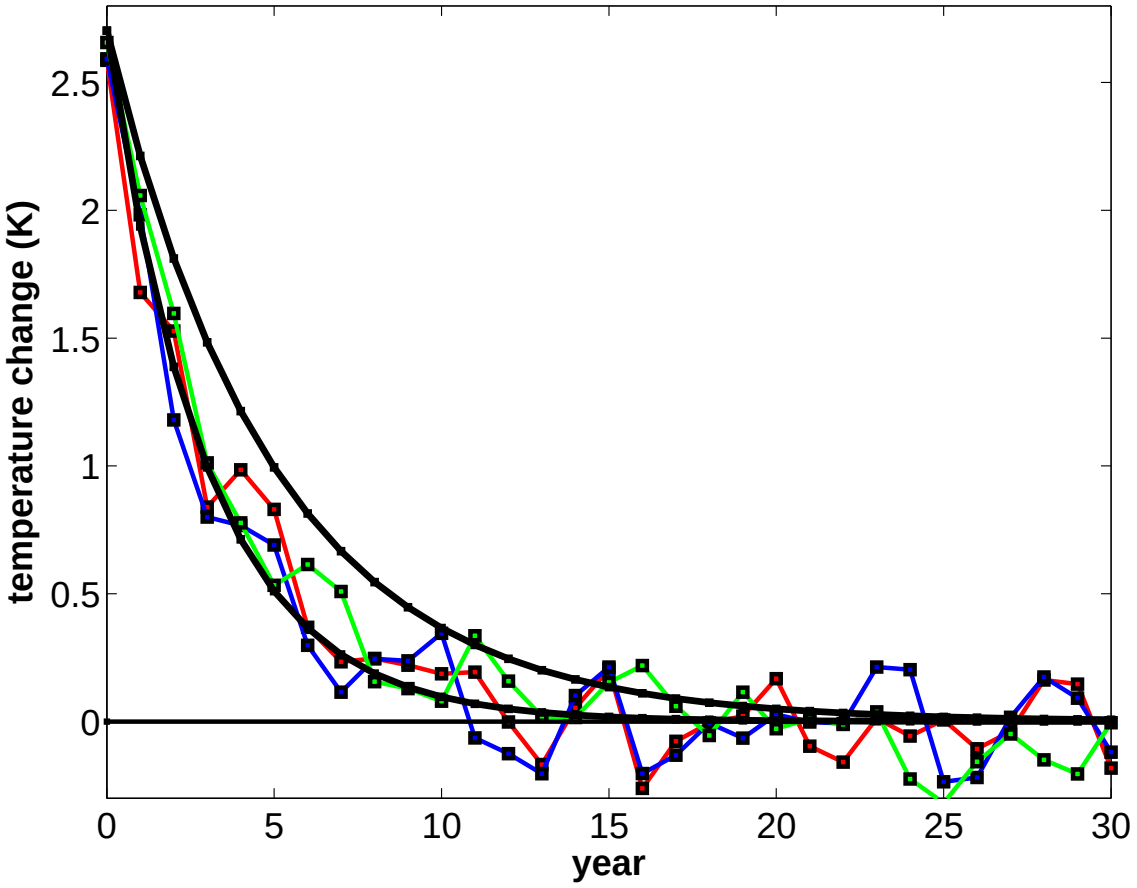

FIG. 5. The initial cooling after instantaneous return of all radiative forcing agents to their values in 1860, with the magnitude of the recalcitrant response subtracted. The three case, switched off in years 2100, 2200 and 2300, are nearly indistinguishable in amplitude as well as temporal evolution. Also shown for reference are exponential relaxation curves with times scales of 3 and 5 years.

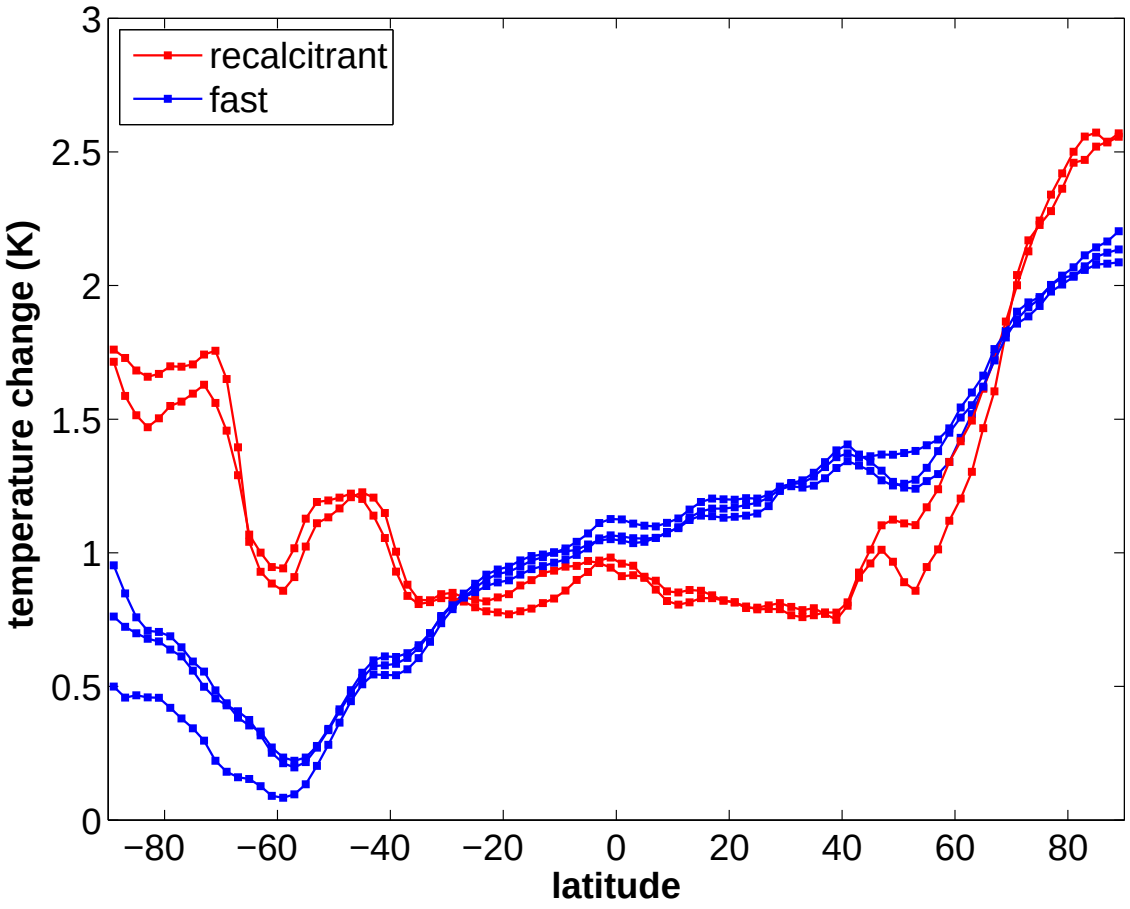

FIG. 6. Structure of the zonal mean response of surface air temperature in the recalcitrant and fast components, normalized so that the global mean of each is unity. Two computations are shown for the recalcitrant component (2200 and 2300) and three for the fast component (2100, 2200, and 2300), as simulated by CM2.1.

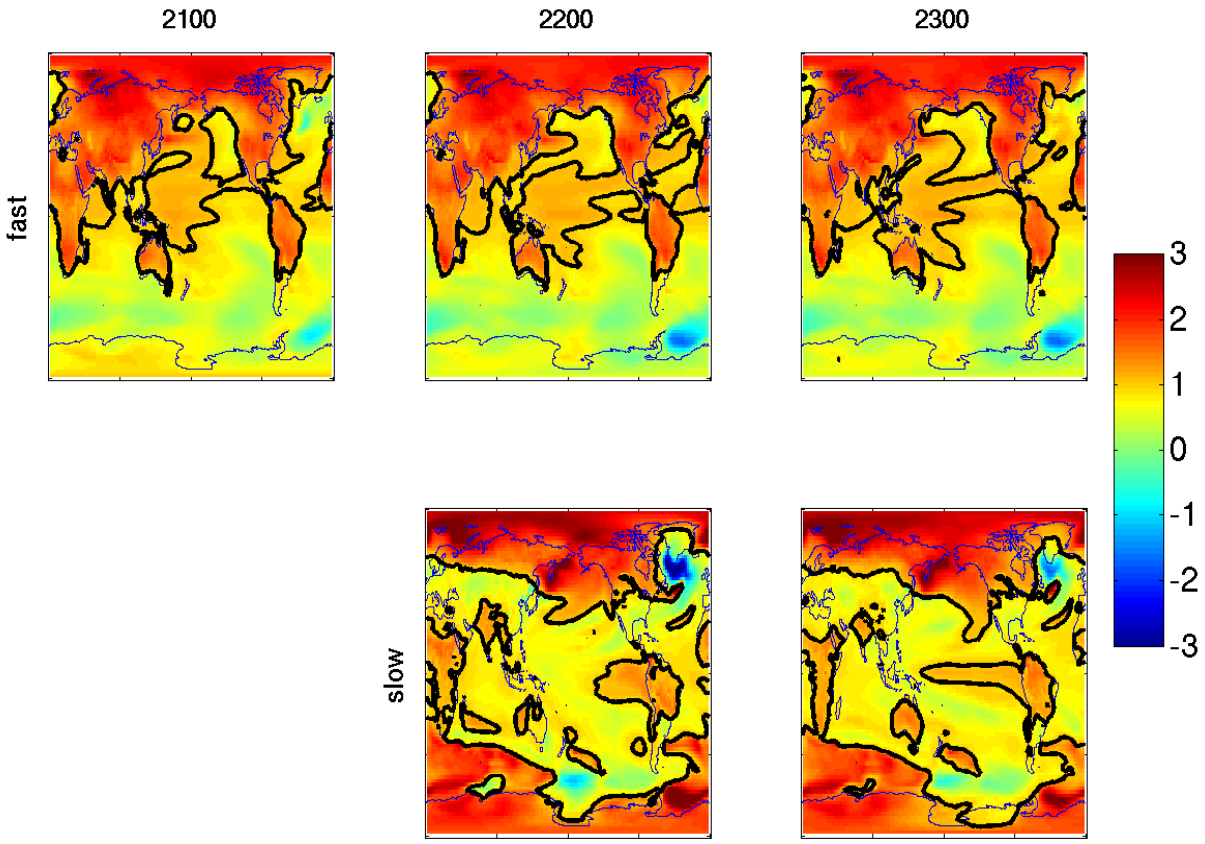

FIG. 7. The spatial pattern of the surface air temperature in the recalcitrant and the fast responses, normalized to unity over the sphere, for the same cases as shown in Fig. 6. The thick contour corresponds to a warming of 1°C, separating those regions with responses larger and smaller than the global mean.